

# RSC Advances



This is an *Accepted Manuscript*, which has been through the Royal Society of Chemistry peer review process and has been accepted for publication.

*Accepted Manuscripts* are published online shortly after acceptance, before technical editing, formatting and proof reading. Using this free service, authors can make their results available to the community, in citable form, before we publish the edited article. This *Accepted Manuscript* will be replaced by the edited, formatted and paginated article as soon as this is available.

You can find more information about *Accepted Manuscripts* in the [Information for Authors](#).

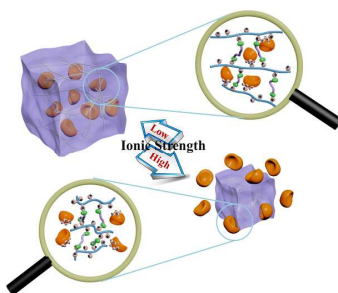
Please note that technical editing may introduce minor changes to the text and/or graphics, which may alter content. The journal's standard [Terms & Conditions](#) and the [Ethical guidelines](#) still apply. In no event shall the Royal Society of Chemistry be held responsible for any errors or omissions in this *Accepted Manuscript* or any consequences arising from the use of any information it contains.

## Table of Contents

### Click Synthesis of Ionic Strength-Responsive Polyphosphazene Hydrogel for Reversible Binding of Enzymes

Yue-Cheng Qian, Peng-Cheng Chen, Xue-Yan Zhu and Xiao-Jun Huang\*

A chemically crosslinkable cationic polyphosphazene was synthesized and fabricated into hydrogels via thiol–ene click chemistry for reversible enzyme binding.



\* To whom all correspondences should be addressed. e-mail: hxjzxh@zju.edu.cn

[Prepared as a Full Paper for Publication in *RSC Advances*]

## **Click Synthesis of Ionic Strength-Responsive Polyphosphazene Hydrogel for Reversible Binding of Enzymes**

Yue-Cheng Qian, Peng-Cheng Chen, Xue-Yan Zhu and Xiao-Jun Huang\*

MOE Key Laboratory of Macromolecular Synthesis and Functionalization,  
Department of Polymer Science and Engineering, Zhejiang University, Hangzhou  
310027, China

---

\* To whom all correspondences should be addressed. e-mail: hxjzxh@zju.edu.cn

## Abstract

In this study, a chemically crosslinkable cationic polyphosphazene was synthesized and fabricated into ionic strength-responsive hydrogels for enzyme binding. This novel polyphosphazene was synthesized via the macromolecular substitution reaction of poly(dichlorophosphazene) with 2-dimethylaminoethylamine, followed by the quaternization to yield the allyl groups. Hydrogels were easily prepared via the thiol–ene click reaction between polyphosphazene and poly(ethylene glycol) dithiol (dithiol PEG) under UV radiation. The inner three-dimensional structure of the hydrogels was investigated by swelling experiments, mechanical property tests, and field emission-scanning electron microscopy. The resulting hydrogels exhibited sensitivity to the ionic strength of the surrounding environment. Lipase from *Candida rugosa* was selected as the model enzyme for the entrapment in these hydrogels, resulting in a maximum enzyme loading of 16.6 mg g<sup>-1</sup> and activity retention as high as 61.6%. Furthermore, the cationic hydrogels were effectively used for reversible enzyme binding owing to the electrostatic interaction, regulated by the ionic strength.

## Introduction

Hydrogels are three-dimensional networked materials that are usually able to imbibe a large amount of water or biological fluids.<sup>1-3</sup> Over the past decade, they have drawn considerable attraction as carriers for enzyme immobilization.<sup>4-7</sup> Enzyme immobilization can overcome the thermal stability, reusability, and recoverability limitations associated with the free enzymes, thus offering feasibilities for continuous operations, significant reduction in operation costs, and simplified product purification process. The hydrated environment in a hydrogel mimics the natural environment of free enzymes, and the entrapped enzymes possess relatively high mobility and flexibility, which is advantageous to their catalytic activity. Besides, the physical and chemical properties of hydrogels can be easily tailored by adjusting the cross-linking density or altering the hydrogel building blocks, which facilitates the construction of high performance enzyme immobilized hydrogels. Hydrogels are also investigated as intelligent materials, exhibiting variations in their volume, structure, and interactions with encapsulated compounds in response to numerous external stimuli including pH,<sup>8</sup> temperature,<sup>9</sup> light,<sup>10</sup> and ionic strength.<sup>11</sup> Among them, hydrogels with ionic strength-responsive behavior show promising applications in biorelated areas such as drug/proteins delivery systems,<sup>12</sup> DNA release systems,<sup>13</sup> and biosensors.<sup>14</sup> Therefore, we envisage that entrapping enzymes in ionic strength-responsive hydrogels can create a favorable process by combining enzyme stability and reuse with supports' responsiveness to ionic strength. From this point of view, it is a prerequisite to include ionic groups in the hydrogel structure.

In general, ionic hydrogels are fabricated by incorporating ionic monomers into the hydrogel network.<sup>15-17</sup> The recent developments in click chemistry have created an

easier and more efficient way to crosslink hydrophilic macromolecules under mild reaction conditions.<sup>18-22</sup> In this context, polymers with both clickable groups and ionic species are required for building of ionic hydrogel blocks.

Polyphosphazenes are a class of hybrid polymers with inorganic elements in the backbone and organic side groups.<sup>23-25</sup> By selecting the appropriate groups attached to the phosphorous atoms, they can be fabricated into materials with diverse forms and functions.<sup>26-31</sup> Due to their flexible synthetic character and tunable physicochemical properties, polyphosphazenes are promising in the field of enzyme immobilization. In principle, ionic polyphosphazene hydrogels can be formed via non-covalent crosslinking and covalent crosslinking. Non-covalent crosslinking is usually based on the ionic induced crosslinking; for example, polyphosphazene with pendant carboxyl groups can be crosslinked through the addition of  $\text{Ca}^{2+}$ . One problem concerned with such non-covalent crosslinked hydrogels is that they are easily disintegrated in monovalent cationic solution.<sup>32</sup> Hydrogels formed by covalent crosslinking exhibit enhanced stabilities, but the simultaneous introduction of covalent crosslinking sites and ionic groups onto the polymer are usually tedious.<sup>33</sup> Therefore, it is desired to find a facile and highly-efficient method to obtain ionic polyphosphazene with clickable groups for covalent crosslinking.

In our previous study, an anionic poly[bis(methacrylate)phosphazene] hydrogel was prepared by nucleophilic substitution and subsequent cross-linking with methacrylic acid, and this hydrogel is used for lipase entrapment.<sup>34</sup> In this study, a cationic clickable polyphosphazene was successfully synthesized by a convenient two-step approach combining nucleophilic substitution and quaternization without traditional protection/deprotection procedures. The corresponding ionic hydrogels were prepared by crosslinking the cationic polyphosphazene and poly(ethylene glycol) dithiol

(dithiol PEG) under UV irradiation. PEG is a biocompatible polymer used in diverse biomedical and biotechnological applications.<sup>35-37</sup> The swelling behavior of the hydrogels in aqueous solutions with varied ionic strength were investigated detailedly. Lipase from *Candida rugosa* was used as the model enzyme for entrapment procedures. Moreover, this type of positively charged hydrogel exhibits reversible enzyme binding ability and therefore is promising in smart enzymatic microreactor systems.

## EXPERIMENTAL

### Materials

Hexachlorocyclotriphosphazene (Bo Yuan New Materials & Technique, Ningbo, China) was purified by recrystallization from heptane and subsequent vacuum sublimation at 60 °C. Poly(dichlorophosphazene) was synthesized via the thermal ring-opening polymerization of the purified hexachlorocyclotriphosphazene in an evacuated Pyrex tube at 250 °C. 2-Dimethylaminoethylamine (DMAEA, 98%, TCI, China), dichloromethane, and triethylamine (TEA) were dried over CaH<sub>2</sub> and distilled prior to use. Allyl bromide (98%, TCI, China), poly(ethylene glycol) dithiol (dithiol PEG, M<sub>n</sub> = 8,000, Sigma-Aldrich) and 2-hydroxy-1-[4-(2-hydroxyethoxy)phenyl]-2-methyl-1-propanone (Irgacure 2959, 98%, TCI, China) were used without further purification. Lipase (from *Candida rugosa*) powders (1,150 units/mg solid), Bradford reagent, and bovine serum albumin (BSA, molecular mass: 67,000 Da) were purchased from Sigma-Aldrich Chemical Co., (St. Louis, MO, USA) and used as received. Fluorescein isothiocyanate-bovine serum albumin (FITC-BSA) (Vector) was used as received. Deionized water used in all the experiments was ultrafiltered to 18.2 MU using an ELGA LabWater system

(Veolia Water Technologies, Paris, France).

### Synthesis of DMAEA-Substituted Polyphosphazene

Poly(dichlorophosphazene) (2.0 g, 17.2 mmol) was dissolved in dry dichloromethane (250 mL), and the resulting solution was added dropwise to a stirred dry dichloromethane (50 mL) solution of DMAEA (7.6 mL, 69.6 mmol) and TEA (9.7 mL, 69.6 mmol) in an ice bath under nitrogen. After an additional 30 min stirring at 0 °C, the reaction mixture was warmed to 25 °C and stirred overnight. The clear solution was dialyzed against 1 M K<sub>2</sub>CO<sub>3</sub> solution for 2 days, and then against water until the solution was not basic anymore (molecular weight cut-off for dialysis membrane: 8–14 kDa) to afford a white and fibrous product after freeze-drying (3.0 g, 80% yield). A single peak was observed by the GPC measurement, where  $M_n = 2.5 \times 10^4 \text{ g mol}^{-1}$ , and the polydispersity index was 1.6.

<sup>1</sup>H NMR (D<sub>2</sub>O, δ): 2.91 (2H, NHCH<sub>2</sub>), 2.43 (2H, NHCH<sub>2</sub>CH<sub>2</sub>), 2.19 (6H, N(CH<sub>3</sub>)<sub>2</sub>).

<sup>31</sup>P NMR (D<sub>2</sub>O, δ): 2.88.

### Synthesis of Allyl-Functionalized Polyphosphazene

1.2 equivalent of allyl bromide (1.9 mL, 21.8 mmol) was added dropwise using a syringe to a solution of DMAEA-substituted polyphosphazene (2.0 g, 9.1 mmol) in 150 mL of absolute methanol at 25 °C. After stirring overnight, the clear solution was dialyzed against water for 5 days, followed by freeze-drying. The final product is white and fibrous (3.8 g, 90% yield).

<sup>1</sup>H NMR (D<sub>2</sub>O, δ): 6.02 (1H, CH<sub>2</sub>=CH), 5.66 (2H, CH<sub>2</sub>=CH), 4.12 (2H, N<sup>+</sup>CH<sub>2</sub>CH), 3.67 (2H, NHCH<sub>2</sub>), 3.34 (2H, NHCH<sub>2</sub>CH<sub>2</sub>), 3.15 (6H, N<sup>+</sup>(CH<sub>3</sub>)<sub>2</sub>). <sup>31</sup>P NMR (D<sub>2</sub>O, δ): 1.05.



## Preparation of Polyphosphazene hydrogels

In a typical experiment, allyl-functionalized polyphosphazene (60 mg, 0.26 mmol double bond), dithiol PEG (50 mg, 0.013 mmol SH), and a photoinitiator (1.5 mg, 0.0065 mmol) were successively dissolved in 1 mL pure water. The clear solution was irradiated under UV light for 10 min to form hydrogels.

## Characterization

$^1\text{H}$  and  $^{31}\text{P}$  NMR spectra were recorded using a Bruker Advance DMX500 in  $\text{D}_2\text{O}$ .  $\text{H}_3\text{PO}_4$  in  $\text{D}_2\text{O}$  was used as the external reference for the  $^{31}\text{P}$  NMR measurements. Molecular weights and molecular-weight distributions were determined by gel permeation chromatography (GPC) using a Waters 208 apparatus equipped with a Waters 2410 RI detector in DMF at 60 °C with polymethylmethacrylate as the calibrant. Fourier transform infrared spectroscopy (FTIR) was performed using a VECTOR 22 spectrometer. The field-emission scanning electron microscopy (FESEM, Hitachi, S4800, Japan) was used to observe the microstructures of the hydrogels. The prepared hydrogel samples were placed in liquid nitrogen for 15 min, fractured mechanically, and then freeze-dried.

## Swelling Behavior and Mechanical Property Measurements

Swelling tests were performed by immersing the freeze-dried hydrogels in 0.05 M phosphate buffer solution (PBS, pH 7.0) or pure water at 25 °C in triplicate. The swollen hydrogels were weighed at regular time intervals after careful removal of the buffer or water on the hydrogel surface. The swelling ratio (SR) of the hydrogels was calculated according to the following equation:

$$\text{SR} = (W_s - W_d)/W_d,$$

where  $W_s$  and  $W_d$  are the weights of the swollen and dry hydrogels, respectively. The compressive stress–strain measurements of the hydrogels were performed on a CHT 4000 electronic universal testing machine (SANS, Shenzhen, China) at a compressive rate of 0.1 mm/min. The cylindrical gel samples were 10 mm in diameter and 5.5 mm in thickness. The storage and loss moduli of hydrogel networks were measured using a rheometer (HR-2, TA Instrument, New Castle, DE) operating at room temperature with a strain amplitude of 0.5%.

### **Lipase Entrapment**

The entrapment of lipase was performed by immersing the hydrogels in lipase solution at 25 °C under reciprocal agitation in water bath. Lipase solution (3.0 mg/mL) was prepared by dissolving lipase powder in PBS (0.05 M, pH 7.0). After the enzyme loading reached equilibrium, the samples were taken out and washed thoroughly with plenty of PBS (0.05 M, pH 7.0) until no free lipase was detected in the washing solution. The enzyme loading was determined using Coomassie brilliant blue reagent following the Bradford's method.<sup>38</sup> BSA was used as the standard to construct a calibration curve. The entrapment capacity of lipase in the hydrogel was calculated from the protein mass balance among the initial and final lipase solutions, and the washings. The enzyme loading was defined as the amount of protein (milligram) per gram of hydrogel. Each reported value was the mean of at least three parallel experiments, and the standard deviation was within ca.  $\pm 5\%$ .

The effect of the ionic strength on mass retention of the lipases immobilized in hydrogels was tested by incubating the lipase-immobilized hydrogels in PBS (0.05 M, pH 7.0) added with different amounts of NaCl, and kept at 25 °C under reciprocal agitation in water bath. At regular time intervals, the lipase concentration in solution

was determined so that the amount of lipase released from the hydrogels can be obtained.

### **Fluorescence Microscopy Observation**

Fluorescence microscopy was used to verify the entrapment of protein within the hydrogels, where FITC-BSA was selected as the model protein. The hydrogels were immersed in a PBS (0.05 M, pH 7.0) solution of FITC-BSA (20.0  $\mu\text{g}/\text{mL}$ ) at 25  $^{\circ}\text{C}$  for 24 h, and then washed thoroughly with plenty of PBS (0.05 M, pH 7.0). After carefully removing the residual buffer on the surface, the hydrogels were cut and the cross section was observed under an emission wavelength of 488 nm. Fluorescence images were recorded using an Eclipse TE2000 optical microscope (Nikon, Japan) equipped with a highly sensitive CCD camera (ORCA-ER, Hamamatsu Photonic, Japan).

### **Assay of Lipase Activity**

The activity of the immobilized lipases was determined using a previously reported method.<sup>39</sup> Briefly, a lipase-immobilized hydrogel was immersed in a reaction mixture composed of 1.0 mL ethanol solution of 14.4 mM *p*-nitrophenyl palmitate and 1.0 mL PBS (0.05 M, pH 7.0) for the enzymatic hydrolysis reaction at 25  $^{\circ}\text{C}$  under reciprocal agitation. After 5 min, the reaction was terminated by withdrawing the lipase-immobilized hydrogel and adding 2.0 mL 0.5 M  $\text{Na}_2\text{CO}_3$  into the mixture, followed by centrifugation at 10,000 rpm for 10 min. A 0.50 mL aliquot of the supernatant was diluted 5-folds with deionized water, and the absorption was measured at 410 nm using a UV-Vis spectrophotometer (UV-2450, Shimadzu, Japan) against a blank without enzyme treated in parallel.

One enzyme unit is defined as the amount of biocatalyst liberating 1.0  $\mu\text{mol}$  *p*-nitrophenol  $\text{min}^{-1}$  for the above conditions. The retention activity value is the ratio of units of immobilized lipase to that of free lipase. Each data is the average of at least three parallel experiments, and the standard deviation was within ca.  $\pm 5\%$ .

### Stability Measurements

The storage stability was determined as follows: free and immobilized lipases were separately stored in PBS (0.05 M, pH 7.0) at 4 °C for 35 days. Parts of them were periodically withdrawn for the activity assay described above. The activity retention of free and immobilized lipase was normalized to their highest activity during the storage period. For the measurement of the thermal stability, both free and immobilized lipases were stored at 60 °C for 240 min. The lipase solution (0.1 mL) or lipase-immobilized hydrogel (5.0 mg) was withdrawn at the same time intervals (30 min) during the incubation, and their residual activity was measured. For the measurement of reusability, the lipase-immobilized hydrogel was withdrawn from the reaction mixture, washed with PBS (0.05 M, pH 7.0) to remove any residual substrate on the hydrogel surface, and then used for the next catalytic assay. The re-immobilization of lipases in the hydrogel was performed by immersing the lipase-immobilized hydrogel in PBS (0.05 M, pH 7.0) containing 1.0 M NaCl until all the immobilized lipases were released, and then the hydrogel was taken out, washed sufficiently by deionized water, dried in air, and finally immersed in a fresh lipase solution until reaching immobilization equilibrium.

## Results and Discussion

### Synthesis of Allyl-Functionalized Cationic Polyphosphazene

Allyl-functionalized cationic polyphosphazene was synthesized by the nucleophilic substitution of poly(dichlorophosphazene) with 2-dimethylaminoethylamine (DMAEA) and subsequent quaternization with allyl bromide. In general, THF is a widely used solvent for the nucleophilic substitution of poly(dichlorophosphazene). However, the tertiary amine group in DMAEA acts as acid acceptor, which can precipitate the polymer during the nucleophilic substitution reaction because of the low solubility of the tertiary amine hydrochloride in THF.<sup>40</sup> Considering this, dichloromethane was used as the reaction solvent to prevent the polymer precipitation.<sup>41</sup> The structures of the resulting polymers were confirmed by <sup>1</sup>H NMR (**Figure S1**) and <sup>31</sup>P NMR (**Figure S2**) spectroscopy. The <sup>31</sup>P NMR spectrum of DMAEA-substituted polyphosphazene showed only one sharp peak, indicating that poly(dichlorophosphazene) was fully substituted, and no side reactions such as rearrangement and hydrolysis occurred. After the quaternization, the signals attributed to protons of DMAEA-substituted polyphosphazene at 2.91, 2.43, and 2.19 ppm disappeared and three new peaks corresponding to these protons appeared at 3.67, 3.34, and 3.15 ppm, indicating that the pendant tertiary amine groups were completely quaternized. The downfield shift of these protons was due to the electron-withdrawing effect of the adjacent quaternary ammonium. The FTIR spectra also indicated the complete quaternization reaction of polyphosphazene (**Figure S3**). The peaks at 2763 and 2858 cm<sup>-1</sup> were attributed to the symmetric stretching vibrations of -CH<sub>3</sub> of the tertiary amine groups, and these peaks disappeared after the quaternization, whereas two bands appeared at 2960 and 3026 cm<sup>-1</sup> were corresponded to the quaternary

ammonium methyl groups.

### Preparation and Characterization of Polyphosphazene Hydrogel

Click chemistry provides a powerful tool for the preparation of functional soft materials.<sup>42-44</sup> In this study, a thiol–ene click reaction was used for the preparation of cationic polyphosphazene hydrogel. This reaction was carried out between the allyl-functionalized polyphosphazene and dithiol PEG in the presence of photoinitiator. Hydrogel (Sample code: Hydrogel 1) was obtained after UV irradiation for 15 min as shown in **Figures 1b** and **1c**. However, the thiol–ene reaction relates to the radical addition reaction, indicating that the hydrogel might also be formed from the direct intermolecular crosslinking among polyphosphazene chains. Therefore, to further investigate the mechanism of the hydrogel formation, three solutions containing different components, namely tertiary amino-functionalized polyphosphazene (Polymer 1)/dithiol PEG/photoinitiator, allyl-functionalized polyphosphazene (Polymer 2)/photoinitiator, and allyl-functionalized polyphosphazene/monothiol OEG/photoinitiator, were exposed to UV light. No hydrogel was observed in these three solutions (**Figures 1d–1f**), verifying that the hydrogel network was constructed through the covalent linkage between the SH groups in dithiol PEG and double bonds in polyphosphazene. Furthermore, FTIR spectroscopy was used to characterize the changes in the chemical structure before and after gelation. The FTIR spectra of the lyophilized Hydrogel 1 and its precursors were shown in **Figure S4**. The peak at  $1635\text{ cm}^{-1}$  in the spectrum of Polymer 2 was assigned to the stretching mode of the double bonds from the allyl group. The peak at  $2594\text{ cm}^{-1}$  in the spectrum of dithiol PEG was due to the adsorption of thiol group. After gelation, adsorption peaks ascribed to thiol groups disappeared. The adsorption

peaks attributed to the double bonds were still observed in the spectrum of Hydrogel 1 because of the excess double bonds in the feed ratio as shown in **Table 1**. Besides, Hydrogels 2 and Hydrogel 3 were prepared by tailoring the feed ratios of allyl-functionalized polyphosphazene and dithiol PEG.

The swelling ratio of hydrogels is a critical parameter for the enzyme entrapment capability. In this study, the swelling behaviors of hydrogels were investigated by gravimetric analysis. **Figure 2a** showed the swelling ratio of the lyophilized hydrogels as a function of time. It can be seen that all these hydrogels reached equilibrium swelling within 18 h. Moreover, the swelling rates and equilibrium swelling ratios of these hydrogels decreased with an increase of the cross-linker content. Nevertheless, hydrogels in PBS (0.05 M, pH 7.0) used for lipase entrapment presented quite different swelling behaviors as shown in **Figure 2b**. All these hydrogels reached equilibrium swelling within only 12 h, and their equilibrium swelling ratios were lower than those in pure water. Similar results were also reported by other researchers.<sup>11,45,46</sup> Swelling property of ionic hydrogels is related to the osmotic imbalance derived from two processes: one is the free exchange between mobile ions inside the gel matrix and the water molecules of the external solution; the other is the electrostatic repulsion between species with the same charge along the polymer chain.<sup>46</sup> Therefore, ionic hydrogels can show remarkable adsorbing ability in pure water. As for a salt solution, the ionic strength reduces not only the osmotic pressure due to the decrease in the concentration difference between the interior hydrogel and the external solution but also the electrostatic repulsion of quaternary ammonium, thus bringing about a decrease in the swelling ratio. The equilibrium swelling ratios of these hydrogels decreased with the increase of the ionic strength in PBS by adding NaCl (**Figure 3**).

The microstructures of freeze-dried hydrogels were characterized by SEM (**Figure 4**), showing interconnected porous networks for all these three hydrogels. The porous structure became more compact with an increase in the cross-linker content, and the average pore size reduced from  $\sim 45 \mu\text{m}$  to  $8 \mu\text{m}$  for Hydrogel 1 and Hydrogel 3, respectively. In general, the smaller pore size in the network structure would keep hydrogel from large deformation.<sup>47</sup> The compressive tests confirmed a positive correlation between cross-linker content and the compressive properties of hydrogels (**Figure S5**). The mechanical properties of hydrogels were also investigated by rheological measurements. Figure 8 showed that all these hydrogels exhibited frequency-independent values for the storage modulus ( $G'$ ) higher than corresponding values for the loss modulus ( $G''$ ), which indicated the formation of stable hydrogels. Besides, the storage modulus of the hydrogels increased with the increase of the cross-linker content.

### **Polyphosphazene Hydrogel for Enzyme Entrapment**

Lipase entrapment in the hydrogels was achieved by immersing the hydrogels in enzyme solutions, where lipase can diffuse in the network of the hydrogel. The curves of the enzyme loading as a function of time were shown in **Figure 6a**. According to this figure, both the enzyme diffusion rate and amount of immobilized enzymes increased when increasing the pore size of hydrogels. The highest enzyme loading was  $16.6 \text{ mg/g}$  for Hydrogel 1 and it was a 25% increase compared to that for Hydrogel 3. Furthermore, the protein distribution was investigated by fluorescence microscopy, where FITC-BSA was selected as the model protein. The fluorescence images of hydrogels after FITC-BSA immobilization showed that FITC-BSA was successfully buried inside the hydrogels (**Figure S6**). As BSA and lipase from



*Candida rugosa* have similar sizes and isoelectric points, lipases can also be immobilized in these hydrogels. The retention activities of the immobilized lipases were listed in **Table 2**. The PEG segments were dexterously contained in the hydrogels, which were biocompatible and can suppress the nonbiospecific interactions between enzyme and support, bringing about activity retentions higher than 50%. Notably, the retention activities of the immobilized lipases showed a pronounced dependence on the hydrogel structure. From Hydrogel 1 to Hydrogel 3, the corresponding retention activity decreased from 61.6% to 52.0%. This result was mainly attributed to an increased mass transfer limitation in the denser network structure that hindered the diffusion of the substrates and products.

The easy leakage of physically encapsulated components is one of the biggest problems for a hydrogel matrix.<sup>48</sup> Notably, in this study, <7% of the encapsulated lipases leaked within 15 h for all the three hydrogels immersed in PBS (0.05 M, pH 7.0) (**Figure 6b**), which was ascribed to the electrostatic interaction between the negatively charged lipases in PBS (0.05 M, pH 7.0) and cationic hydrogels. Ionic strength of the aqueous environment can affect this interaction. To further clarify the effect of the ionic strength on the immobilization stability, the lipase-immobilized hydrogels were placed in PBS (0.05 M, pH 7.0) with various amounts of NaCl added and the corresponding mass retention of the encapsulated lipases was investigated. According to **Figure 7**, the mass retention decreased with the increase in ionic strength. The hydrogels retained 55% to 75% of the original amount of the immobilized lipases after being immersed in PBS (0.05 M, pH 7.0) with NaCl concentration of 0.2 M for 12 h, whereas nearly all lipases were washed away within 30 min by increasing the NaCl concentration to 2.0 M. In addition, the leakage rate decreased from Hydrogel 1 to Hydrogel 3, which was due to the decrease of pore size

that helped to confine the lipases.

The storage and thermal stability are significant issues for practical application of biocatalysts.<sup>49</sup> In this study, both the storage and thermal stability of free and immobilized lipases were studied, as plotted in **Figure 8**. **Figure 8a** showed that the immobilized lipases displayed lower decay rate compared to the free lipases. Furthermore, a first-order kinetic model was used to estimate the lifetime of lipases.<sup>50</sup> The corresponding fitting results were listed in **Table 2**, indicating that the immobilized lipases exhibited extended half-lives ranging from 10 d to 19 d, as compared to 6 d for free lipases. This result indicated that a denser network structure can better protect the lipases and lead to an improved storage stability. A similar trend was also observed for the thermal stability test shown in **Figure 8b**. The half-life increased from 1.7 h for the free lipases to 5.4 h for those immobilized in Hydrogel 3.

These cationic hydrogels are promising in smart enzymatic microreactor systems. For example, lipases were entrapped in Hydrogel 3 to fabricate this enzyme-immobilized microreactor because of its lowest percentage of enzyme leakage. After seven cycles of batch operation of hydrolyzing *p*-nitrophenyl palmitate, >60% of the original activity still remained (**Figure 9**). While in our previous work, >55% of enzyme activity was lost in anionic poly[bis(methacrylate)phosphazene] hydrogel after only four cycles of batch operation, which was mainly due to the loss of entrapped lipases.<sup>34</sup> Then, the encapsulated lipases were released from the hydrogel at high ionic strength. The regenerated hydrogel were reused for enzyme immobilization via immersing it in a fresh lipase solution. The same washing process was performed at the initial stage of another four rounds of immobilization. According to **Figure 9**, the activities of the fresh immobilized lipases and the corresponding activity decay curve in each of the following four rounds were similar to those in the first round, indicating

that the hydrogel network remained nearly intact during these batch operations.

## Conclusions

Cationic polyphosphazene hydrogels were designed and fabricated for lipase immobilization. Allyl-functionalized cationic polyphosphazene synthesized via macromolecular nucleophilic substitution and quaternization processes was crosslinked by dithiol PEG under UV irradiation. The resulting hydrogels exhibited ionic strength responsive property, and their equilibrium swelling ratios decreased with an increase in ionic strength of the aqueous environment. The mechanical strength of the hydrogels increased gradually when increasing crosslinker amount, whereas their pore sizes decreased. Lipase immobilization results indicated that the pore size significantly affected the enzyme loading and the activity retention of the immobilized enzymes. Interestingly, the immobilized lipases can be released from the hydrogels by increasing the ambient ionic strength, which was due to a reduced electrostatic interaction between enzymes and hydrogels. The regenerated hydrogel can be repeatedly used for enzyme immobilization. Taken together, these results verified the feasibility of applying these cationic hydrogels in smart enzymatic microreactor systems.

## Acknowledgement.

This work was supported by the National Natural Science Foundation of China (Grant No. 21274126), National "Twelfth Five-Year" Plan for Science & Technology Support of China (No. 2012BAI08B01).

## References

- [1] Q. G. Wang, J. L. Mynar, M. Yoshida, E. J. Lee, M. S. Lee, K. Okuro, K. Kinbara and T. Aida, *Nature*, 2010, **463**, 339–343.
- [2] A. M. Kloxin, A. M. Kasko, C. N. Salinas and K. S. Anseth, *Science*, 2009, **324**, 59–63.
- [3] E. A. Appel, X. J. Loh, S. T. Jones, F. Biedermann, C. A. Dreiss and O. A. Scherman, *J. Am. Chem. Soc.*, 2012, **134**, 11767–11773.
- [4] M. H. Kim, S. An, K. Won, H. J. Kim and S. H. Lee, *J. Mol. Catal. B: Enzym.*, 2012, **75**, 68–72.
- [5] F. L. Qu, Y. Zhang, A. Rasooly and M. H. Yang, *Anal. Chem.*, 2014, **86**, 973–976.
- [6] R. Sato, T. Kawakami and H. Tokuyama, *React. Funct. Polym.*, 2014, **76**, 8–12.
- [7] N. Milašinović, N. Milosavljević, J. Filipović, Z. Knezević-Jugović and M. K. Krušić, *Polym. Bull.*, 2012, **69**, 347–361.
- [8] H. Bai, C. Li, X. L. Wang and G. Q. Shi, *Chem. Commun.*, 2010, **46**, 2376–2378.
- [9] H. J. Dai, Q. Chen, H. L. Qin, Y. Guan, D. Y. Shen, Y. Q. Hua, Y. L. Tang and J. Xu, *Macromolecules*, 2006, **39**, 6584–6589.
- [10] K. Peng, I. Tomatsu and A. Kros, *Chem. Commun.*, 2010, **46**, 4094–4096.
- [11] S. G. Roy and P. De, *Polymer*, 2014, **55**, 5425–5434.
- [12] M. Dadsetan, Z. Liu, M. Pumberger, C. V. Giraldo, T. Ruesink, L. C. Lu and M. J. Yaszemski, *Biomaterials*, 2010, **31**, 8051–8062.
- [13] A. Agarwal, R. C. Unfer and S. K. Mallapragada, *Biomaterials*, 2008, **29**, 607–617.
- [14] G. Lin, S. Chang, C. H. Kuo, J. Magda and F. Solzbacher, *Sens. Actuators, B Chem.*, 2009, **136**, 186–195.
- [15] M. Das and E. Kumacheva, *Colloid. Polym. Sci.*, 2006, **284**, 1073–1084.

- [16] J. E. Elliott, M. Macdonald, J. Nie and C. N. Bowman, *Polymer*, 2004, **45**, 1503–1510.
- [17] Y. L. Luo, K. P. Zhang, Q. B. Wei, Z. Q. Liu and Y. S. Chen, *Acta Biomater.*, 2009, **5**, 316–327.
- [18] Y. J. Jiang, J. Chen, C. Deng, E. J. Suuronen and Z. Y. Zhong, *Biomaterials*, 2014, **35**, 4969–4985.
- [19] J. K. Zheng, L. A. S. Callahan, J. K. Hao, K. Guo, C. Wesdemiotis, R. A. Weiss and M. L. Becker, *ACS Macro Lett.*, 2012, **1**, 1071–1073.
- [20] T. Cai, W. J. Yang, Z. B. Zhang, X. L. Zhu, K. G. Neoh and E. T. Kang, *Soft Matter*, 2012, **8**, 5612–5620.
- [21] F. Yu, X. D. Cao, Y. L. Li, L. Zeng, B. Yuan and X. F. Chen, *Polym. Chem.*, 2014, **5**, 1082–1090.
- [22] D. A. Ossipov and J. Hilborn, *Macromolecules*, 2006, **39**, 1709–1718.
- [23] H. R. Allcock, *Soft Matter*, 2012, **8**, 7521–7532.
- [24] S. Lakshmi, D. S. Katti and C. T. Laurencin, *Adv. Drug Deliv. Rev.*, 2003, **55**, 467–482.
- [25] R. D. Jaeger and M. Gleria, *Prog. Polym. Sci.*, 1998, **23**, 179–276.
- [26] A. Singh, N. R. Krogman, S. Sethuraman, L. S. Nair, J. L. Sturgeon, P. W. Brown, C. T. Laurencin and H. R. Allcock, *Biomacromolecules*, 2006, **7**, 914–918.
- [27] I. Teasdale, S. Wilfert, I. Nischang and O. Bruggemann, *Polym. Chem.*, 2011, **2**, 828–834.
- [28] S. C. Lee and J. Y. Chang, *Macromolecules*, 2009, **42**, 5402–5405.
- [29] K. Maeda, K. Kuroyanagi, S. Sakurai, T. Yamanaka and E. Yashima, *Macromolecules*, 2011, **44**, 2457–2464.

- [30] L. Hu, A. Q. Zhang, K. Liu, S. Lei, G. X. Ou and X. J. Chen, *RSC Adv.*, 2014, **4**, 35769–35776.
- [31] A. K. Andrianov, *J. Inorg. Organomet. Polym. Mater.*, 2006, **16**, 397–406.
- [32] H. R. Allcock and S. Kwon, *Macromolecules*, 1989, **22**, 75–79.
- [33] H. R. Allcock, S. R. Pucher, M. L. Turner and R. J. Fitzpatrick, *Macromolecules*, 1992, **25**, 5573–5577.
- [34] Y. C. Qian, P. C. Chen, G. J. He, X. J. Huang and Z. K. Xu, *Molecules*, 2014, **19**, 9850–9863.
- [35] R. Banerjee, S. Gupta, D. Dey, S. Maiti and D. Dhara, *React. Funct. Polym.*, 2014, **74**, 81–89.
- [36] Z. Liu, J. T. Robinson, X. M. Sun and H. J. Dai, *J. Am. Chem. Soc.*, 2008, **130**, 10876–10877.
- [37] J. A. Burdick and K. S. Anseth, *Biomaterials*, 2002, **23**, 4315–4323.
- [38] M. Bradford, *Anal. Biochem.*, 1976, **72**, 248–254.
- [39] X. J. Huang, P. C. Chen, F. Huang, Y. Ou, M. R. Chen and Z. K. Xu, *J. Mol. Catal. B Enzym.*, 2011, **70**, 95–100.
- [40] H. R. Allcock, M. B. McIntosh, E. H. Klingenberg and M. E. Napierala, *Macromolecules*, 1998, **31**, 5255–5263.
- [41] Y. Akgöl, C. Hofmann, Y. Karatas, C. Cramer, H. D. Wiemhöfer and M. Schonhöff, *J. Phys. Chem. B*, 2007, **111**, 8532–8539.
- [42] A. J. Qin, J. W. Y. Lam and B. Z. Tang, *Macromolecules*, 2010, **43**, 8693–8702.
- [43] A. B. Lowe, *Polym. Chem.*, 2014, **5**, 4820–4870.
- [44] R. K. Iha, K. L. Wooley, A. M. Nystöm, D. J. Burke, M. J. Kade and C. J. Hawker, *Chem. Rev.*, 2009, **109**, 5620–5686.

- [45] F. K. Li and H. Li, *Soft Matter*, 2010, **6**, 311–320.
- [46] X. X. Liu, Z. Tong and O. Hu, *Macromolecules*, 1995, **28**, 3813–3817.
- [47] Y. Lee, D. N. Kim, D. K. Choi, W. J. Lee, J. W. Park and W. G. Koh, *Polym. Adv. Technol.*, 2008, **18**, 852–858.
- [48] R. A. Sheldon and S. Pelt, *Chem. Soc. Rev.*, 2013, **42**, 6223–6235.
- [49] K. P. Dhake, A. H. Karoyo, M. H. Mohamed, L. D. Wilson and B. M. Bhanage, *J. Mol. Catal. B Enzym.*, 2013, **87**, 105–112.
- [50] J. P. Henley and A. Sadana, *Enzyme Microb. Technol.*, 1985, **7**, 50–60.

Table 1 Sample codes for all the prepared hydrogels

Sample code	Double bond:SH:PI (mole ratio)	Polymer 2 concentration (mg mL <sup>-1</sup> )	Reaction time (min)
Hydrogel 1	1:0.05:0.025	60	15
Hydrogel 2	1:0.1:0.05	60	15
Hydrogel 3	1:0.18:0.09	60	15



Table 2 Parameters of the free and immobilized lipases

Samples	Enzyme loading (mg g <sup>-1</sup> )	Activity retention (%)	Half-lives of lipases at 60 °C (h)	Half-lives of lipases stored at 4 °C (d)
Free lipase	–	100	1.7	6
Lipase immobilized in Hydrogel 1	16.6	61.6	3.7	10
Lipase immobilized in Hydrogel 2	15.0	55.2	4.6	13
Lipase immobilized in Hydrogel 3	13.2	52.0	5.4	19

## Figure Captions:

**Scheme 1.** Schematic presentation of the synthesis of polyphosphazene derivatives and preparation of hydrogel. Polyphosphazene with pendant allyl groups were synthesized via the quaternization of polyphosphazene with pendant tertiary amino groups by allyl bromide. The thiol–ene reaction between polyphosphazene with pendant allyl groups and poly(ethylene glycol) (PEG) dithiol was conducted in aqueous solution with UV irradiation up to 15 min.

**Figure 1.** Photographs of polymer solutions before (a) and after UV irradiation (b)–(f). (a)–(c): allyl-functionalized polyphosphazene (polymer 2)/dithiol PEG/photoinitiator (PI) (Molar ratio of double bond/SH/PI: 1/0.05/0.025), (d) tertiary amino-functionalized polyphosphazene (polymer 1)/dithiol PEG/PI (Molar ratio of tertiary amine/SH/PI: 1/0.05/0.025), (e) polymer 2/PI (Molar ratio of double bond/PI: 1/0.025), (f) polymer 2/monothiol OEG/PI (Molar ratio of double bond/SH/PI: 1/0.05/0.025)

**Figure 2.** Swelling curves of the hydrogels in (a) pure water and (b) PBS (0.05 M, pH 7.0).

**Figure 3.** Effect of the amounts of NaCl added in PBS (0.05 M, pH 7.0) on the equilibrium swelling ratios of the hydrogels. An illustrative graphical representation for three-dimensional network structure of the ionic hydrogels under different ionic strength conditions is inserted.

**Figure 4.** SEM micrographs of (a) Hydrogel 1, (b) Hydrogel 2 and (c) Hydrogel 3. The scale bars represent 100  $\mu\text{m}$ , and all images were recorded at identical magnification.

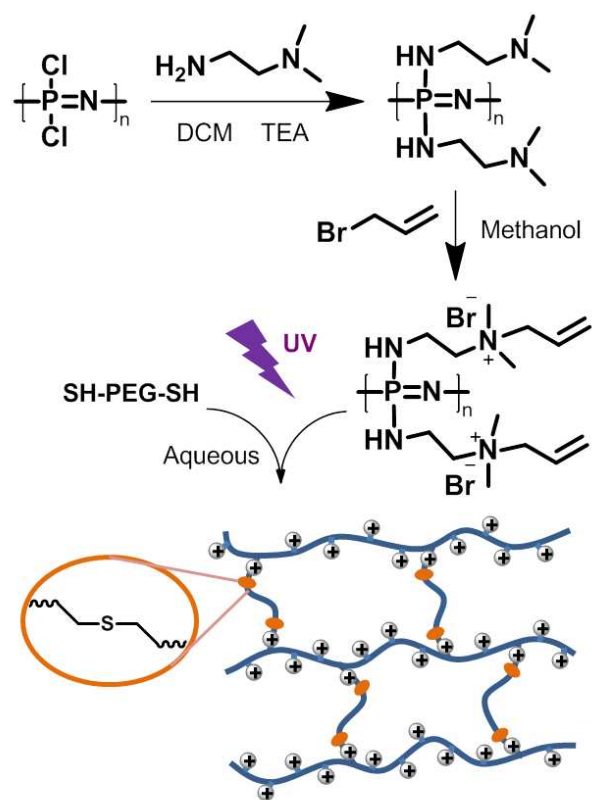
**Figure 5.** Storage modulus  $G'$  (closed circle) and loss modulus  $G''$  (open circle) of hydrogels as a function of frequency in the oscillatory frequency sweep.

**Figure 6.** (a) Enzyme loading for hydrogels and (b) mass retention of the lipases immobilized in hydrogels after being washed by PBS (0.05 M, pH 7.0).

**Figure 7.** Mass retention of the lipases immobilized in the hydrogels after being washed by PBS (0.05 M, pH 7.0) containing different amounts of NaCl.

**Figure 8.** (a) Storage activities of the free and immobilized lipases stored in PBS (0.05 M, pH 7.0) at 4 °C and (b) thermal stabilities of the free and immobilized lipases incubated in PBS (0.05 M, pH 7.0) at 60 °C. The fitting lines were drawn to determine their respective storage and thermal half-lives.

**Figure 9.** Reusability of the immobilized lipases. The arrow indicates that the hydrogel was washed in a solution containing 0.05 M phosphate buffer and 1.0 M NaCl to remove the encapsulated lipase and subsequently immersed in fresh lipase solution for a new round of immobilization. The same washing process was performed at the initial stage of each round of immobilization.



Scheme 1

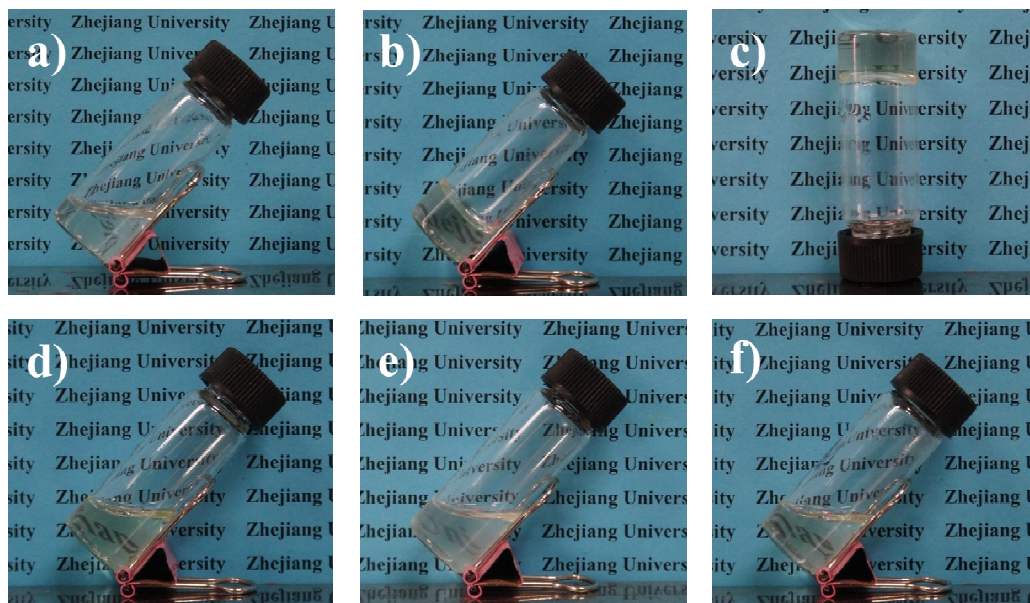


Figure 1

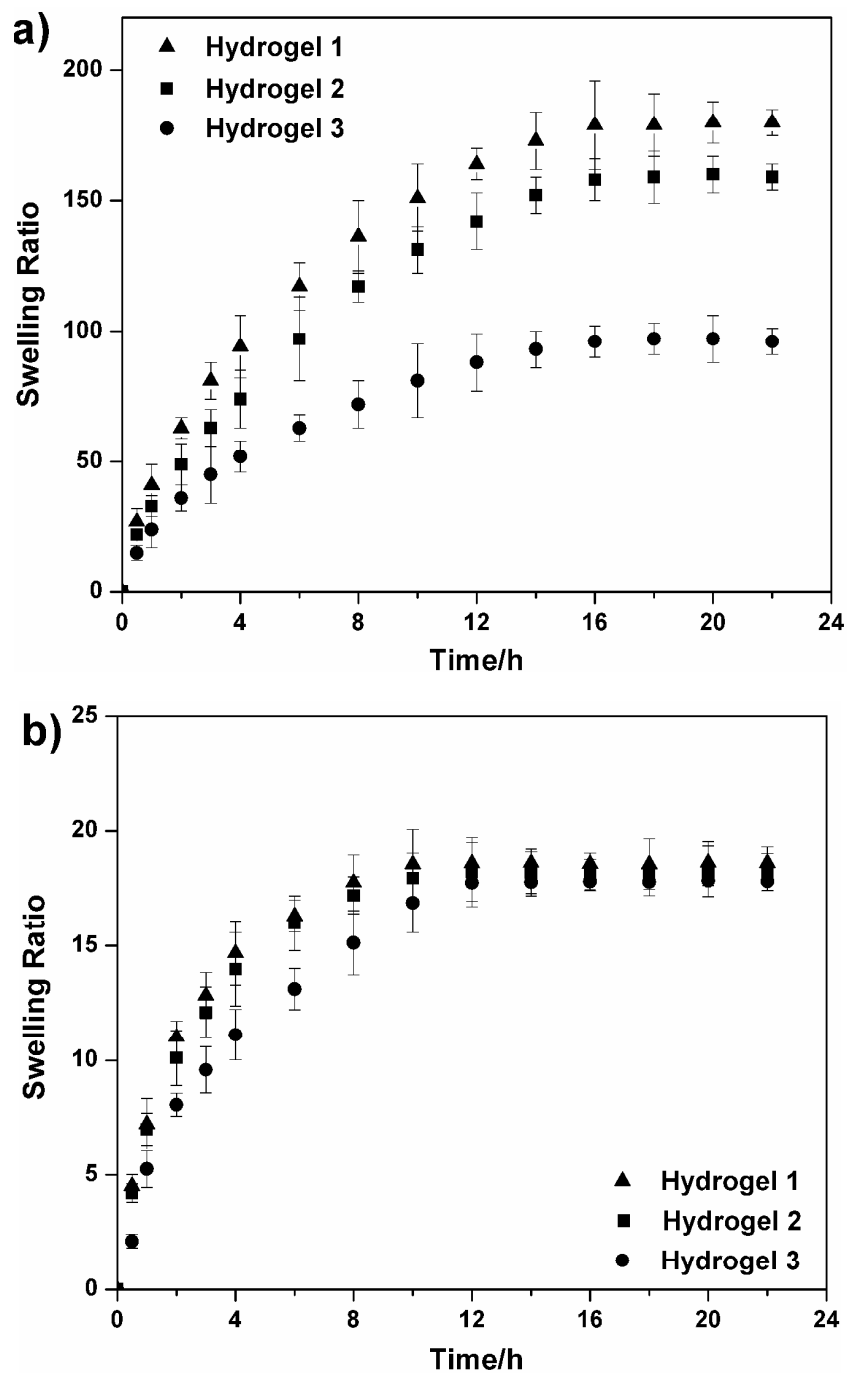


Figure 2

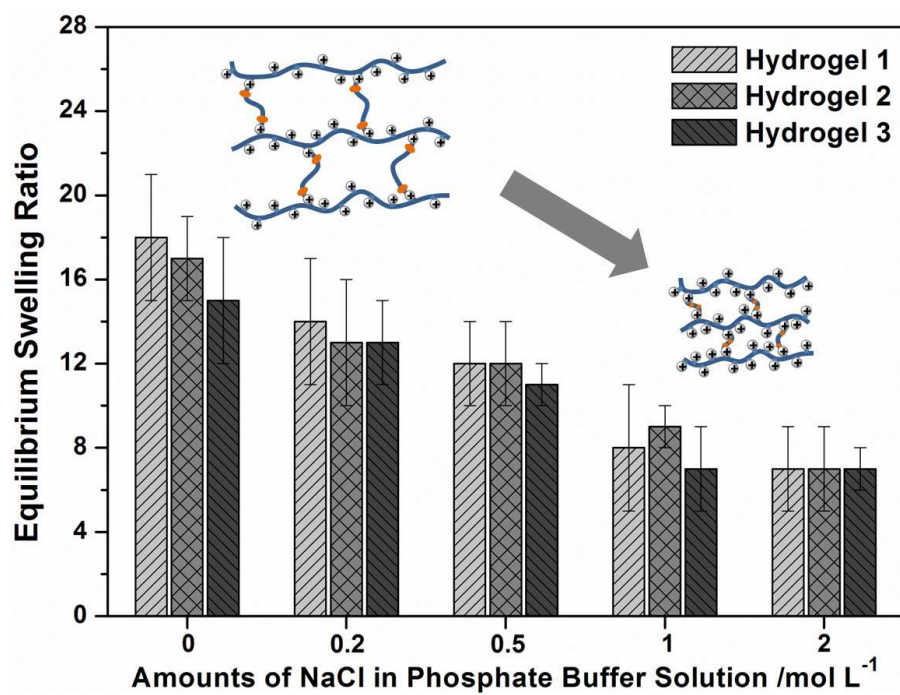


Figure 3

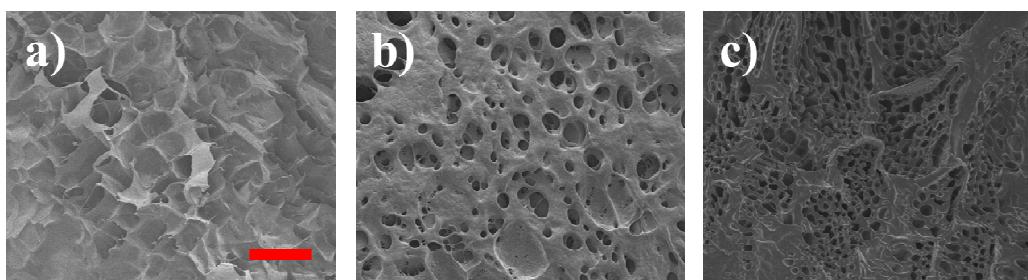


Figure 4



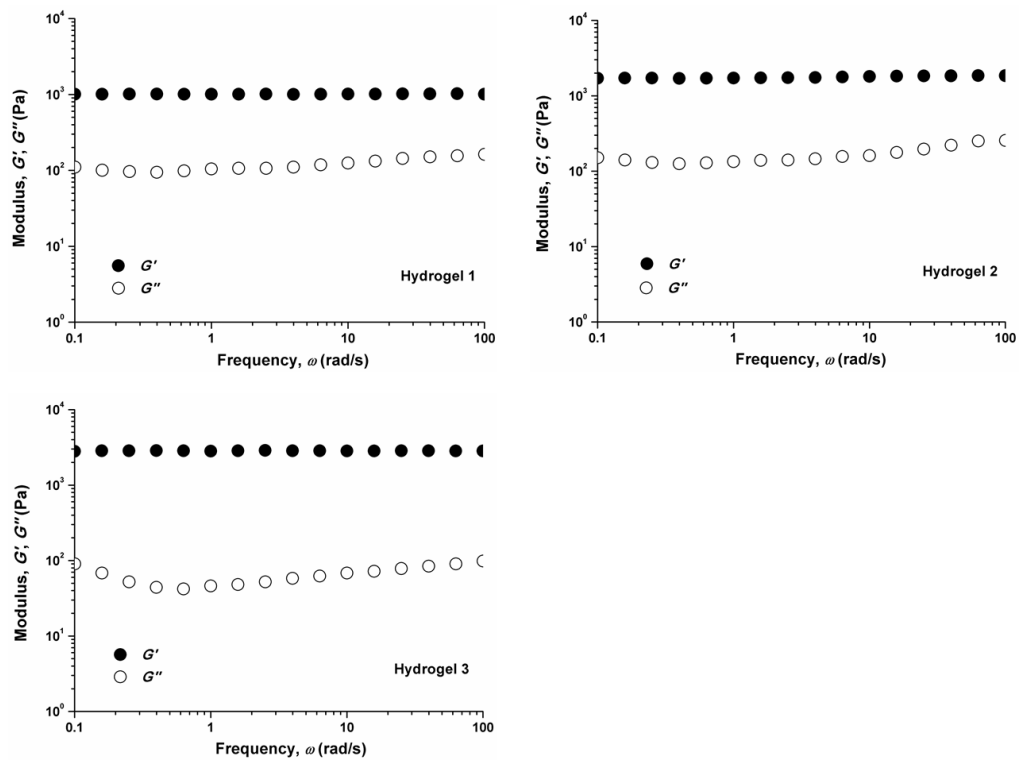


Figure 5

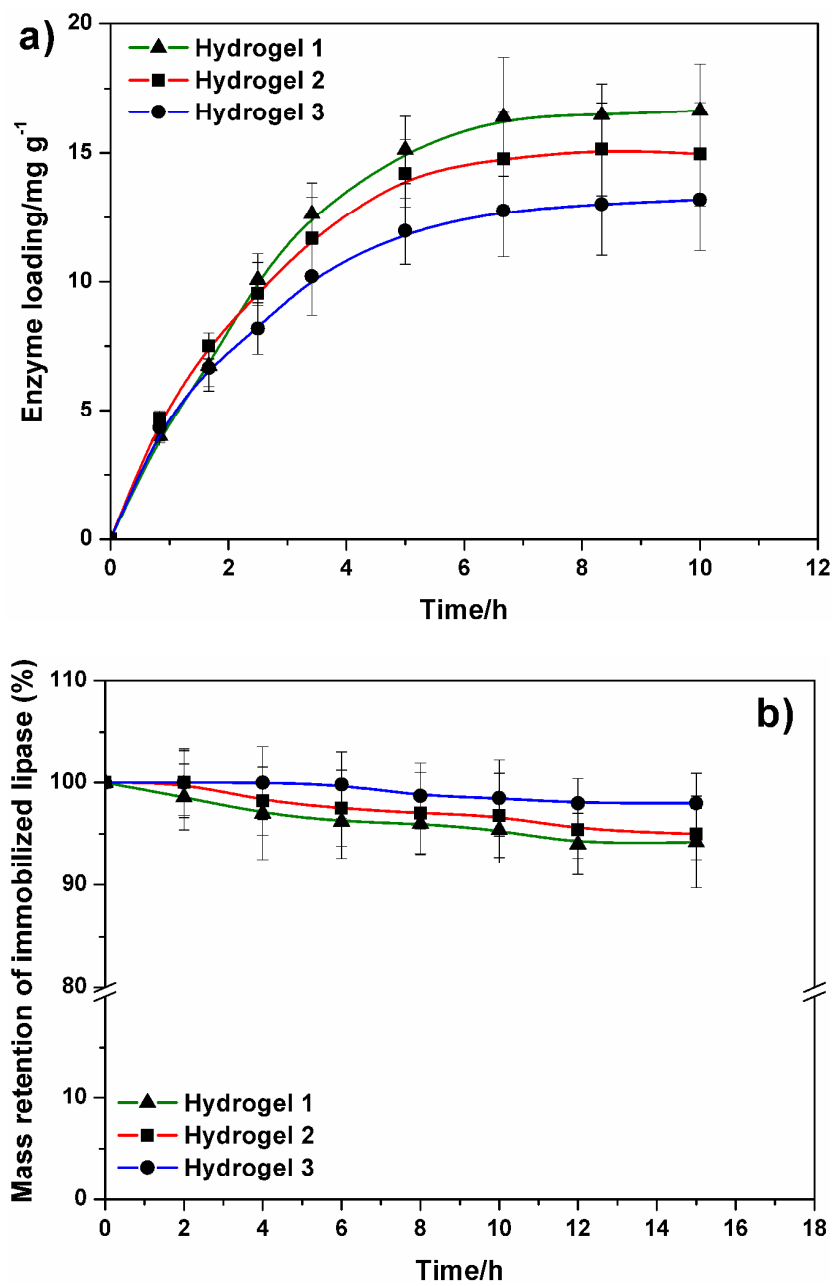


Figure 6

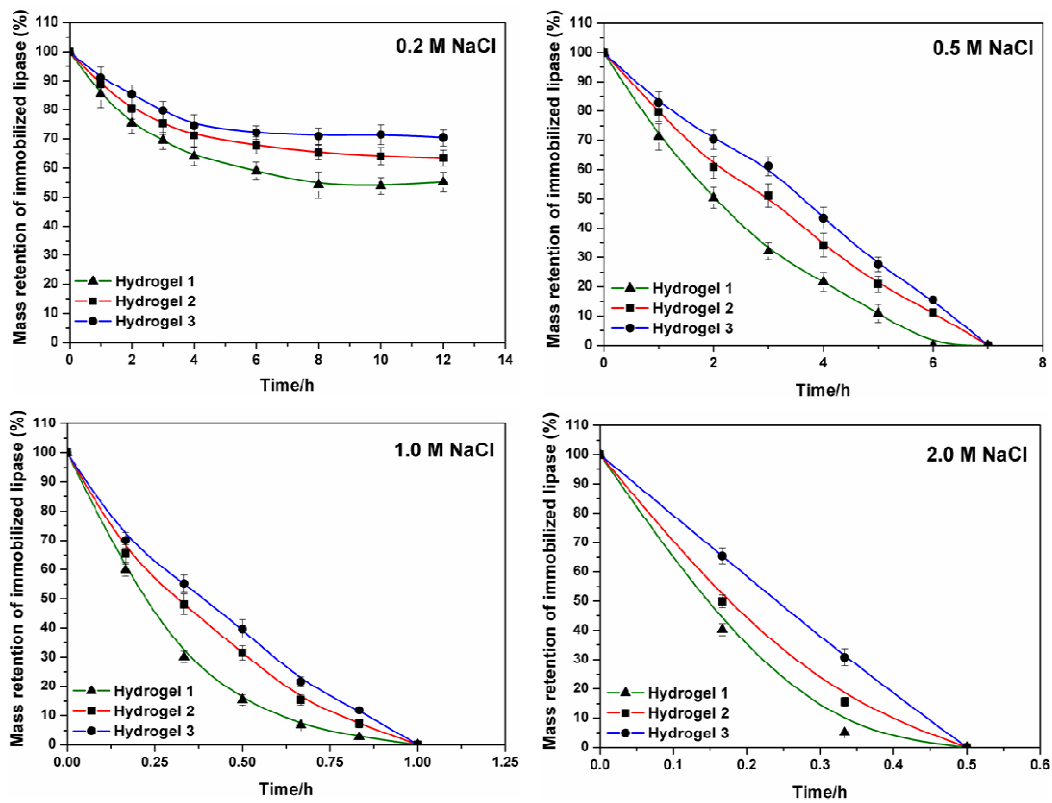


Figure 7

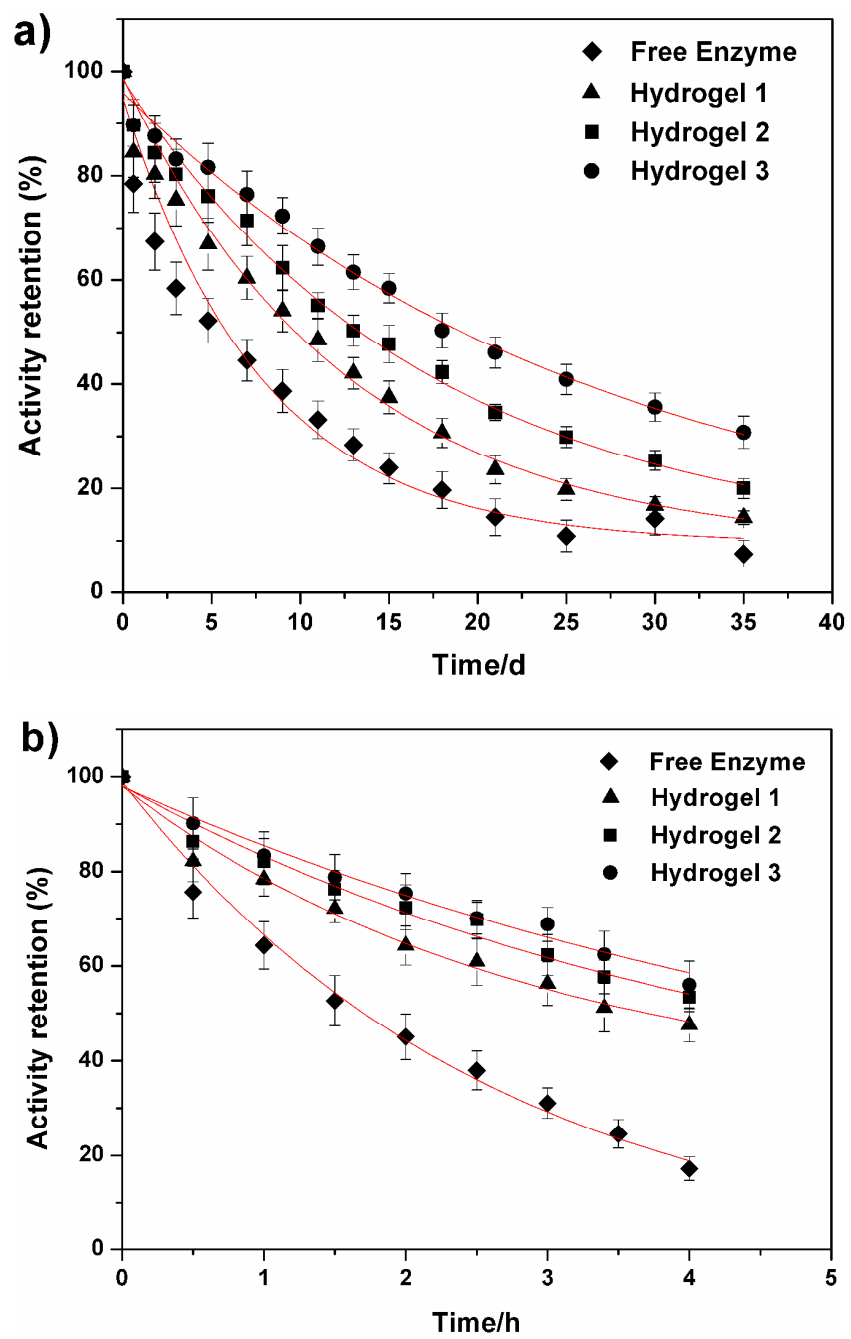


Figure 8

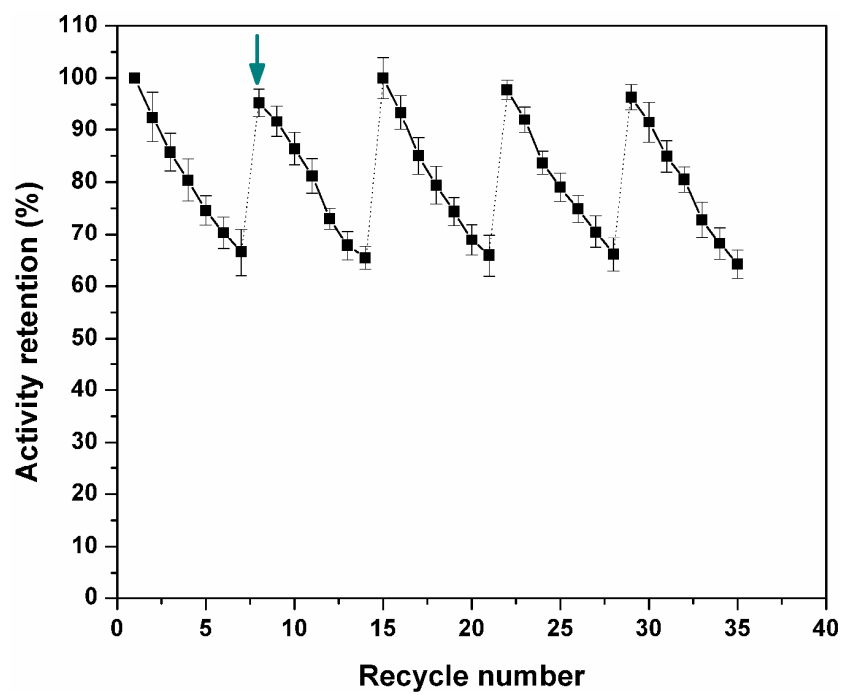


Figure 9